

Adaption of the LHC cold mass cooling system to the requirements of the Future Circular Collider (FCC)

C Kotnig^{1,2}, L Tavian¹, G Brenn²

¹ CERN, Geneva, Switzerland

² Graz University of Technology, Graz, Austria

E-mail: claudio.kotnig@cern.ch

Abstract. The cooling of the superconducting magnet cold masses with superfluid helium (He II) is a well-established concept successfully in operation for years in the LHC. Consequently, its application for the cooling of FCC magnets is an obvious option. The 12-kW heat loads distributed over 10-km long sectors not only require an adaption of the magnet bayonet heat exchangers but also present new challenges to the cryogenic plants, the distribution system and the control strategy. This paper recalls the basic LHC cooling concept with superfluid helium and defines the main parameters for the adaption to the FCC requirements. Pressure drop and hydrostatic head are developed in the distribution and pumping systems; their impact on the magnet temperature profile and the corresponding cooling efficiency is presented and compared for different distribution and pumping schemes.

1. Introduction

The purpose of the cold mass cooling is to maintain the superconducting state of the coils by keeping them at a temperature below a certain limit (≈ 2 K). Four different heat sources affecting the cold mass were taken into account: beam gas scattering (dynamic), resistive heating in the coil splices (dynamic), heat transfer through the cold bore (semi-dynamic) and heat leaks from the ambience (static). In nominal operation at maximal beam energy, an average heat load of 1.38 W/m was estimated. For margin, the installed capacity is designed to run the cold mass cooling dependably at a possible heat load of 2.44 W/m.

2. Cooling Concept

Figure 1 illustrates structure and operating principle of the cold mass cooling of one half-cell, a cryogenic unit of seven magnets in series ($\cong 107.1$ m). The 8400 m long beam bending section is supplied with single-phase normalfluid helium branched from the supply header C (\varnothing 80 mm, 4.6 K and 3 bar). The He II two-phase flow is delivered to the half-cell's end by a smaller feeder pipe integrated in the bayonet heat exchanger [1]. When returning, the liquid He II is evaporated, extracting heat from the cold mass. The entirely evaporated flow exiting the bayonet heat exchanger is discharged in the return header B to be led back to the cryoplant.

To avoid exergy losses, liquid entrainment in the returning two-phase helium must be reduced by keeping the flow in the (smooth) stratified flow regime. Vapour velocities up to 5 m/s are possible to suppress the generation of wrested droplets from the liquid helium surface [2]. To avoid overflow in steady-state operation, the liquid helium must be evaporated before it reaches



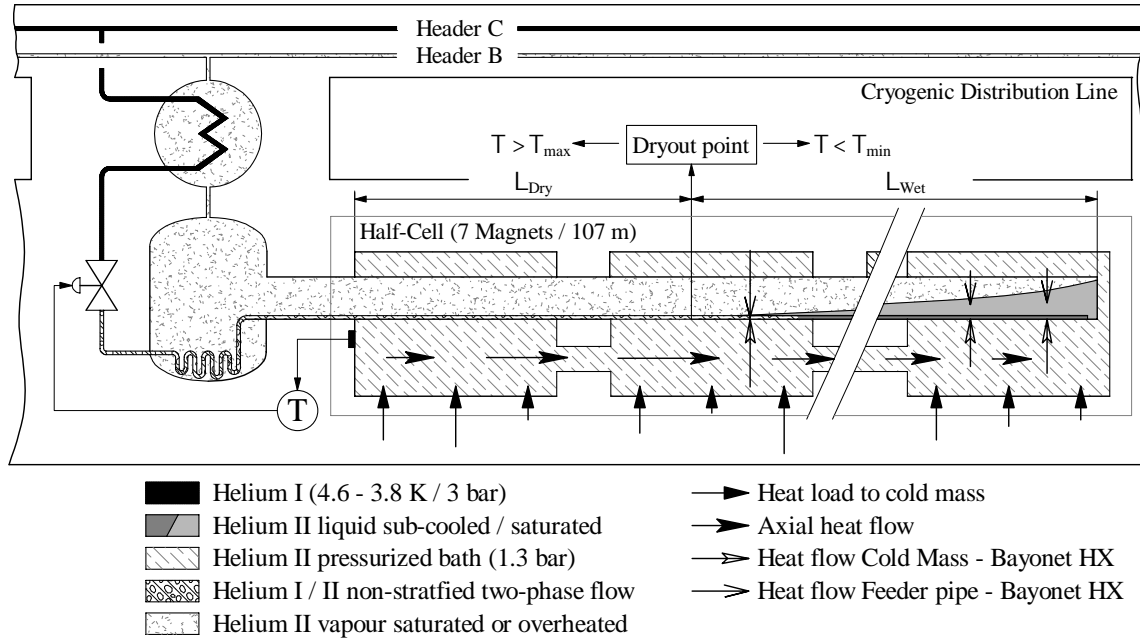


Figure 1. Structure and operating principle of the cold mass cooling of one FCC half-cell with superfluid helium in a bayonet heat exchanger.

the separator dividing the bayonet heat exchanger into a dry section (dry length L_{Dry}) and into a section containing liquid helium (wetted length L_{Wet}). The system's control variable is the cold mass temperature of the warmest magnet close to the separator. The beam pipes containing the hadron beams run in parallel to the bayonet heat exchanger and are not depicted in figure 1.

3. Stratified flow modelling

Mass (1), momentum (2) and energy (3) balance equations were solved for each phase, where only the steady-state operation was considered. The subscript Φ can be substituted with the phase identifiers *Liq* and *Vap*. Figure 2 graphically shows the effects and geometrical parameters taken into account to model the stratified flow in the bayonet heat exchanger. The helium flow in the feeder pipe was modelled as homogeneous flow if it was in the two-phase regime [3].

3.1. Mass

The generated vapour mass due to evaporation is the product of the total helium flow rate \dot{m} and the change of the vapour mass fraction dx (the plus sign indicates the equation for the vapour phase, the minus sign for the liquid phase). v denotes the average velocity in the flow cross section and ρ the average density of the corresponding phase.

$$\frac{d}{dz} (A_{\Phi} \rho_{\Phi} v_{\Phi}) = \pm \dot{m} \frac{dx}{dz} \quad (1)$$

3.2. Momentum

If any slope occurs, the cryogen passes the half-cell in descending direction. The pressure of the two-phase flow was assumed to be constant over the entire flow cross section. The shear stresses between the pipe wall and the fluids were calculated with the Fanning friction factor $f_{P\Phi}$ derived by the formula of Churchill, the interfacial shear stress was calculated according

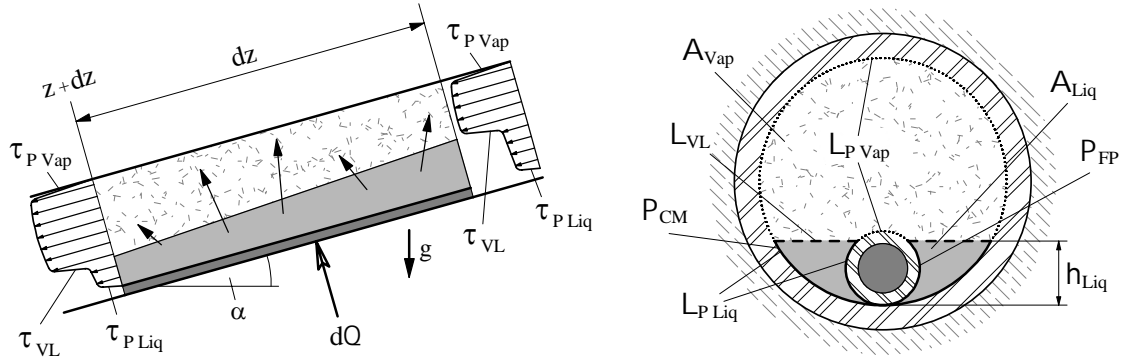


Figure 2. *Left:* Inclined piece of the bayonet heat exchanger of length dz .

Right: Surfaces and perimeters for the pressure drop calculation of bayonet heat exchanger stratified flow and perimeters contributing to the radial heat transfer between stratified flow and the static helium bath and the stratified flow and the feeder pipe flow.

to [4]. A denotes the cross section area, L_P denotes the length of a pipe's perimeter wetted by the corresponding phase, L_{VL} denotes the length of the interface between the two phases and τ the corresponding shear stresses. In the momentum and in the wall friction terms, the plus sign corresponds to the liquid phase, the minus sign to the vapour phase.

$$\underbrace{\dot{m}_\Phi \frac{dv_\Phi}{dz}}_{\text{Change of momentum}} = \underbrace{-A_\Phi \frac{dp}{dz}}_{\text{Pressure forces}} \underbrace{\mp \tau_{VL} L_{VL} - \tau_{P\Phi} L_{P\Phi}}_{\text{Friction forces}} + \underbrace{g \rho_\Phi A_\Phi \sin \alpha}_{\text{Weight}} - \underbrace{\dot{m} \frac{dx}{dz} \Delta v_{VL}}_{\text{Evaporation}} \quad (2)$$

$$\Delta v_{VL} = 0 \quad \dots \text{for the liquid phase}$$

$$\Delta v_{VL} = v_{vap} - v_{liq} \quad \dots \text{for the vapour phase}$$

3.3. Energy

Only thermal energies were taken into account in the energy balance and the longitudinal heat conduction in the liquid phase was neglected. Radial heat transfer from the cold mass and from the feeder pipe flow to the stratified flow were assumed. $(h'' - h')$ denotes the latent heat of the evaporated helium, \dot{q}_{CM} and \dot{q}_{FP} denote the heat fluxes transferred to the stratified flow from the cold mass and the feeder pipe in W/m^2 .

$$(h'' - h') dx = \frac{\dot{q}_{CM} P_{CM} + \dot{q}_{FP} P_{FP}}{\dot{m}} dz \quad (3)$$

4. Heat extraction from the cold mass

The heat absorbed by the helium vapour is negligible as almost the entire heat load has to be extracted by the liquid helium. The areas taken into account for the radial heat transfer are shown in figure 2 on the right-hand side. The heat conducted tangentially along the dry parts of the copper pipes was quantified to be several orders of magnitude smaller than the heat transferred radially where the pipes are wetted and therefore is neglected in the framework of this paper. The heat load along the dry section must be conducted axially to the wetted part of the bayonet heat exchanger inside the cold mass. The cold mass is immersed in a static pressurized bath (1.3 bar) of superfluid helium, in which the heat is transferred radially and axially to the bayonet heat exchanger [5].

4.1. Radial heat transfer

The copper pipes were assumed to have a temperature-independent thermal conductivity (88 W/(m·K)). For temperatures around 2 K, the thermal resistivity between the liquid helium and the copper pipe wall is mainly driven by the Kapitza resistance [3]. After exiting the Joule-Thomson valve, the helium temperature exceeds the λ -temperature, and the heat transfer coefficient was calculated to obtain the thermal resistivity.

The superfluid helium between the iron yoke laminations transfers the heat very well due to the thermomechanical effect. The radial temperature gradient is on the order of 10^{-2} mK/m making the helium bath temperature dependent on the axial coordinate z only. The temperature difference between the superconducting coil and the helium bath was calculated to be not higher than 50 mK based on a preliminary cos Θ -design of the coils.

4.2. Axial heat transfer

The axial heat transfer due to the thermomechanical effect is impeded by friction. Hence the entire heat load on the dry length must be conducted to the wetted part of the bayonet heat exchanger. The one-dimensional heat conduction in superfluid helium can be calculated with (4). An empirically obtained formula to calculate the thermal conductivity function $1/f_k$ of superfluid helium depending on temperature and pressure was used [3].

$$\frac{dT}{dz} = -f_k \dot{q}^m \quad (4)$$

where dT/dz is obtained in K/m with f_k in (m^{5.8} K)/W^{3.4} and \dot{q} in W/m². The exponent m has the value of 3.4.

5. Numerical simulation

The inner diameter of the bayonet heat exchanger was calculated not to exceed a velocity of 5 m/s when operating at the installed capacity. The pressure drop in the heat exchanger was determined to be 1 mbar for the maximal flow rate operating at the installed capacity and was decreased accordingly for smaller helium flow rates ($\propto \dot{m}^2$). To enable controlling without overflow, a minimal dry length of 20 % of the half-cell length was determined as margin. A lower limit for the suction pressure of the discharged helium vapour of 15 mbar (p_{Bmin}) was set. The maximal slope of the FCC is expected to be ± 0.6 % and the cryogenic distribution system is designed to have a descending stratified flow in each half-cell independent of its location. Table 1 summarizes geometrical data and presumed values not discussed in the former text.

Table 1. Geometrical values and boundary conditions

Variable	Unit	Symbol	LHC	FCC
Half-cell length	m	L_{HC}	106.9	107.1
Average heat load nominal (installed) capacity	W/m	\dot{q}	0.40 (0.83)	1.38 (2.44)
Bayonet HX inner diameter	mm	d_{Baj}	53.4	83.1
Feeder pipe inner diameter	mm	d_{FP}	10.0	15.0
Thickness bayonet HX pipe wall	mm	t_{Baj}	2.3	5.0
Joule-Thomson valve inlet temperature	K	T_{JTin}	2.18	2.18
Heat load on header B	W/m	\dot{Q}_B	0.11	0.24

Equations (1)–(4) were discretized and a one-dimensional numerical simulation performed. By choosing boundary conditions, the special solutions of the set of equations may be determined. The geometrical values (A, L, P) in figure 2 and the phase velocities can be expressed as functions

of the liquid level h_{Liq} in the bayonet heat exchanger. It was assumed for the two phases to generate the same longitudinal pressure drop in each element Δz (0.1 m).

6. Cold mass cooling of one half-cell

The diagrams in figure 3 illustrate exemplarily the temperature and heat transfer profiles in a half-cell. ① marks the dryout point, where also the inflection points of the temperature profiles of the helium bath and the maximal axial heat flux occur. At the half-cell's end, the heat flux extracted from the cold mass is high due to the large wetted perimeter of the bayonet heat exchanger (②). With decreasing liquid level and increasing cold mass temperature, the heat flux profile shows a convex shape with a local minimum (③). Close to the dryout point, the driving temperature difference increases causing a high heat transfer before it suddenly vanishes due to the total evaporation of the helium (④). The heat flux entering from the feeder pipe is large, corresponding to the high driving temperature difference - after passing a short distance, the feeder pipe flow is liquefied entirely, and the temperature is assimilated to the stratified flow temperature (⑤).

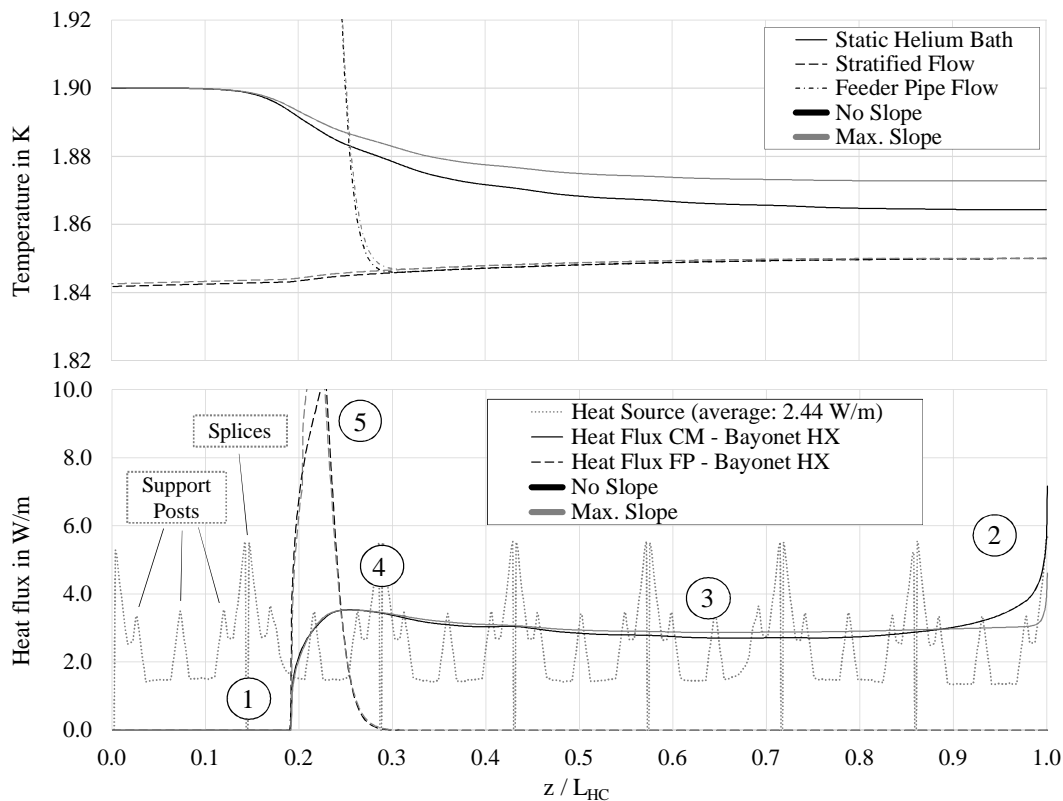


Figure 3. Temperature profiles for the static helium bath, the stratified flow and the feeder pipe flow (top) and heat flux from the static helium bath to the bayonet heat exchanger, from the feeder pipe flow to the bayonet heat exchanger, and the heat load (bottom) vs. the axial coordinate z/L_{HC} with and without slope, a maximal bath temperature of 1.9 K and operating at the installed capacity.

Figure 4 shows the required free area in the cold mass to conduct the heat axially, depending on the difference between the maximal bath temperature and the feeder pipe outlet temperature for three cold mass temperature levels, with and without slope, operating at the installed capacity. The half-cells located in inclined sectors provide the critical design parameters for

the cold mass cooling system. The effect of the cold mass temperature on the required free area is of secondary order compared to the influence of the available temperature range.

In the LHC the difference between the maximal bath temperature and the feeder pipe outlet temperature reaches about 50 mK with a free area of 60 cm². To yield the same temperature difference in the FCC, the available free area must be accordingly larger. Based on the preliminary cold mass design a free area of 156 cm² was determined.

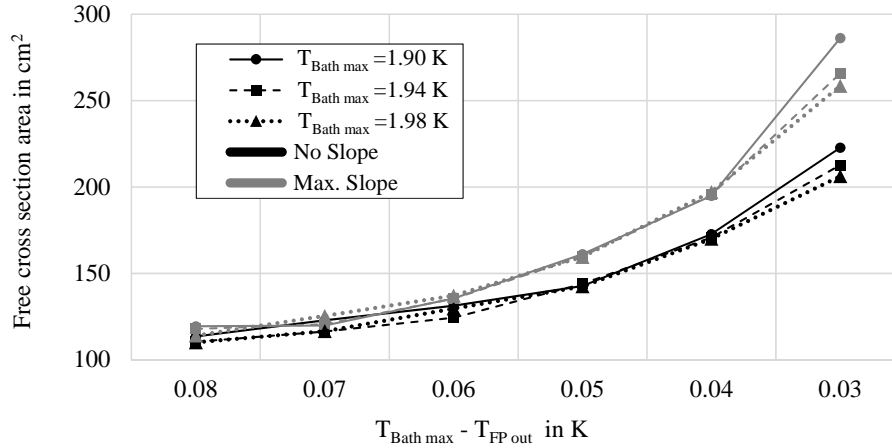


Figure 4. Required free cross section area vs. the difference between the maximal bath temperature $T_{Bath\ max}$ and the feeder pipe outlet temperature $T_{FP\ out}$ for three different temperature levels, with and without slope, operating at the installed capacity.

7. Cold mass cooling of one FCC long sector

One FCC long cryogenic sector consists of 79 half-cells (≈ 8400 m) cooled in series. The pressure in the bayonet heat exchanger of the last half-cell and the pressure progress in the return header B dictate the operation temperature of all the previous half-cells. The critical design case of the cold mass cryogenic distribution system is an ascending vapour flow returning to the cryoplant, since the frictional and gravitational pressure losses sum up. The diagram in figure 5 shows the maximal bath temperature (of the last half-cell) as a function of the necessary diameter of the header B for a suction pressure of 15 mbar ($p_{B\ min}$).

The exergetic efficiency ζ of the sector cooling and distribution is indirectly proportional to the helium bath temperature limit $T_{Bath\ max}$ and the difference of the specific exergies Δe_{CB} of the entering and exiting helium flows. T_a denotes the ambient temperature.

$$\zeta \propto \left(\frac{T_a}{T_{Bath\ max}} - 1 \right) \frac{1}{\Delta e_{CB}} \quad (5)$$

The maximum bath temperature is a requirement set by the superconducting coils. The specific exergy contained in the returning helium vapour is mainly a function of the suction pressure in header B, whose final value is determined by three design parameters:

- (i) The maximum bath temperature determines the theoretical minimal saturation temperature in the bayonet heat exchangers.
- (ii) The free area in the cold mass determines the difference between the maximum bath temperature and the feeder pipe outlet temperature in the last half-cell.
- (iii) The header B diameter determines the pressure drop in the header B and therefore the saturation pressure of all half-cells except the last one.

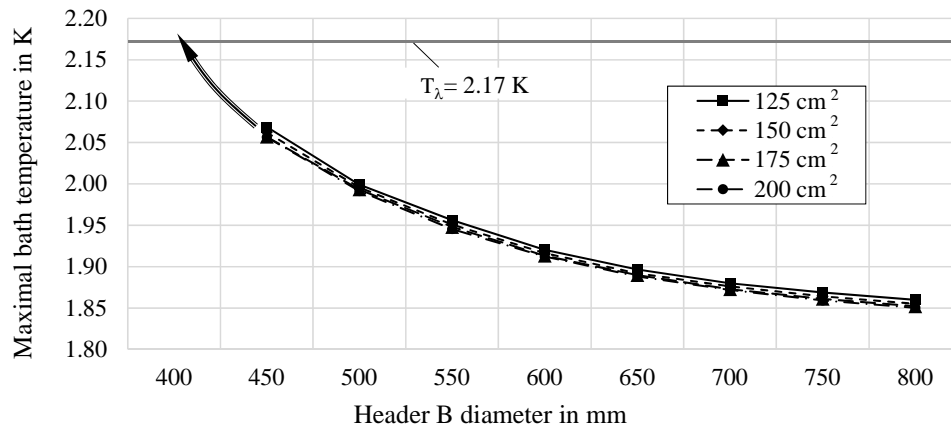


Figure 5. Maximum bath temperature (of the last half-cell) of an inclined sector vs. the header B diameter operating at the nominal capacity for four different free areas and a suction pressure of 15 mbar.

Large header B diameters and free areas approximate the suction pressure and the pressures in the bayonet heat exchangers and therefore increase the exergetic efficiency [6]. Figure 6 shows the correlation of the pressure profile in header B and the saturation temperature in the half-cells. The decreasing pressure in header B causes a sub-cooling of all half-cells except the last one below the necessary temperature limit.

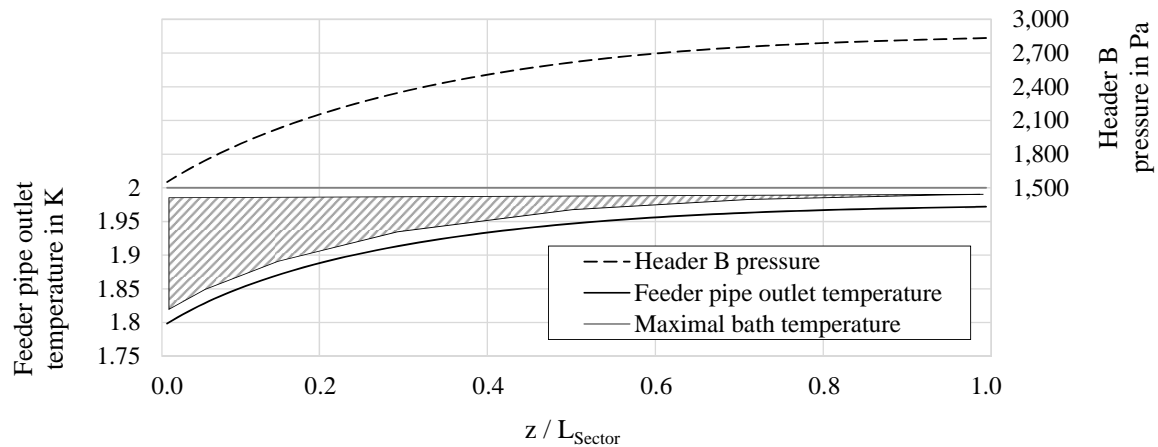


Figure 6. Feeder pipe outlet temperature and header B pressure profiles in an inclined sector vs. the axial coordinate z/L_{Sector} for a maximal bath temperature of 1.995 K, a free area of 156 cm² and a header diameter of 500 mm, operating at the nominal capacity; the height of the hatched area represents the difference between the cold mass temperature and its technical and theoretical minimum.

The baseline foresees a diameter of 500 mm for the header B. The graphs in the diagram in figure 5 yield the possible combinations of free area and helium bath temperature limit. If none of these combinations are acceptable for the magnet design, the header diameter must be increased or additional machinery to transport the helium vapour has to be installed. Three options are presented and schematically illustrated in figure 7:

- 1) The installation of high speed compressors or blowers along the cryogenic distribution line.

- 2) Splitting of the helium vapour flow and compression of one partial flow in an additional cold compressor station installed at the sector end (a) or in the middle of the sector (b).
- 3) Splitting of the helium vapour flow and compression of one partial flow in an additional warm compressor station installed at the sector end.

The separated helium flow of the options (2) and (3) has to be conveyed back in an additional header (G) at cryogenic temperature level and should not increase the size of the cryogenic distribution line. The assembly of additional machinery generates additional capital (machines, pipes, civil engineering) and operational costs and decreases the exergetic efficiency.

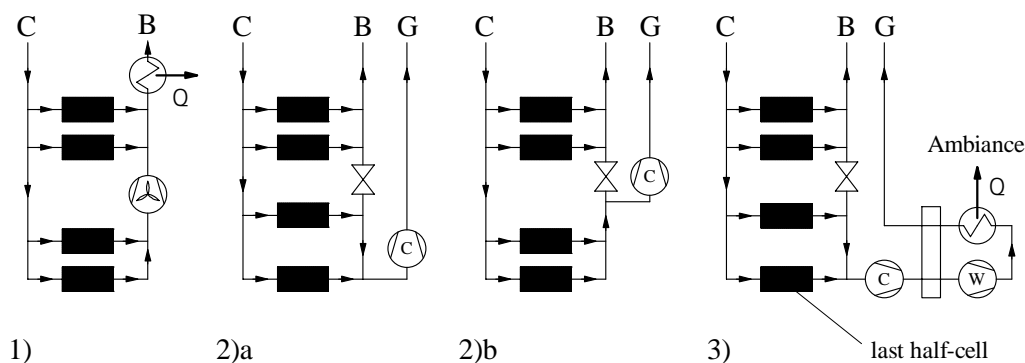


Figure 7. Three possibilities of additional machinery to return the helium vapour to the cryoplants to avoid an enlargement of the cryogenic distribution line.

8. Conclusion

To operate the cold mass cooling efficiently, a minimal length of the dry section in the bayonet heat exchanger was determined. The axial heat transfer along the dry section creates a temperature difference, whose value mainly depends on the free section in the cold mass filled with superfluid helium. The available space for cryogenics in the cold mass and the temperature limit of the superconducting coils determine a minimal return line diameter to keep the pressure of the helium vapour flow above a required value of 15 mbar. Space restrictions limit the size of the cryogenic distribution line, but an eventual enlargement of the return header B can be circumvented by additional machinery to transport the helium vapour to the cold compressor stations. The investigation of the feasibility and the resulting costs of eligible extensions of the cryogenic distribution systems is the next step in the FCC cryogenic distribution design phase.

References

- [1] Lebrun P, Serio L, Taviani L and van Weelderden R 1997 *Cooling Strings of Superconducting Devices below 2 K: The Helium II Bayonet Heat Exchanger*. Advances in Cryogenic Engineering Vol **43**. pp. 419 – 426
- [2] di Muio E, Jager B, Puech L, Rousset B, Thibault P, van Weelderden R, Wolf PE 2002 *Optical investigations of He II two phase flow*. AIP Conference Proceedings **613**, pp. 1675 – 1682
- [3] Van Sciver S 2012 *Helium Cryogenics*. Springer, New York
- [4] Grimaud L, Gauthier A, Rousset B and Delhay J M 1997 *Stratified two-phase superfluid helium flow: II**. Cryogenics, Vol **37**, issue 11. pp. 742 – 744
- [5] Lebrun P and Taviani L 2013 *Cooling with Superfluid Helium*. Proceedings of the CAS-CERN Accelerator School: Superconductivity for Accelerators, 2013, April 24 - May 4, Erice
- [6] Kotnig C, Taviani L and Brenn G 2017 *Investigation and performance assessment of hydraulic schemes for the beam screen cooling for the Future Circular Collider of hadron beams*. IOP Conference Series **171** 012006